

## C-Slot Circular Polarized Antenna for Hybrid Energy Harvesting and Wireless Sensing

Irfan Mujahidin<sup>1</sup>, Sidiq Syamsul Hidayat<sup>1\*</sup>, Muhamad Cahyo Ardi Prabowo<sup>2</sup> and Akio Kitagawa<sup>3</sup>

<sup>1</sup>Department of Telecommunication Engineering, Faculty of Electrical Engineering, Semarang State Polytechnic, Semarang 50275, Indonesia

<sup>2</sup>Department of Electronic Engineering, Faculty of Electrical Engineering, Semarang State Polytechnic, Semarang 50275, Indonesia

<sup>3</sup>Department of Electrical Engineering and Computer Science, Kanazawa University, Ishikawa 9201192, Japan

### ABSTRACT

This paper presents a new hybrid energy harvesting on electromagnetic solar for wireless energy harvesting of ambient from sensors of low-power devices. The axial ratio (AR) requirements produce Left-Hand Circular Polarization (LHCP) and Right-Hand Circular Polarization (RHCP) and simultaneously produce a 90-degree phase difference during energy harvesting, adopting a new design in designing a dual-feed broadband circular polarized (CP) antenna. To get the frequency band 2.3–2.4 GHz, we propose a C-Slot antenna with a circular patch dual feed. To estimate the diversity of the phase and magnitude output of the feed configuration under AR value, we used a 50 Ohm feed network output of the characteristic analysis for a dual feed CP antenna. An Axial ratio frequency range of less than 3 dB is achieved using polarization analysis with different branch channel couplers. To produce a DC output voltage, a high-frequency rectifier circuit embedded with a thin-film solar cell on the antenna is then connected to two T-junction power divider rectifiers, resulting in a high-efficiency design. A complete system-level analysis will include multiple signal classification methods of powered ambient RF energy using a wireless energy harvesting array that proposes a compact structure and demonstrates

optimal configuration. Reliable operation in typical indoor environments indicates a self-contained sensor Node. Therefore, it has significant implications for powering small electronics and wireless sensor applications independently of the IoT Network or real implementation telecommunications industry.

**Keywords:** CP antenna, hybrid energy harvesting, wireless sensing

### ARTICLE INFO

#### Article history:

Received: 16 August 2023

Accepted: 02 November 2023

Published: 04 April 2024

DOI: <https://doi.org/10.47836/pjst.32.3.24>

#### E-mail addresses:

[irfan.mujahidin@polines.ac.id](mailto:irfan.mujahidin@polines.ac.id) (Irfan Mujahidin)

[sidiqsh@polines.ac.id](mailto:sidiqsh@polines.ac.id) (Sidiq Syamsul Hidayat)

[m.cahyoardi.p@polines.ac.id](mailto:m.cahyoardi.p@polines.ac.id) (Muhamad Cahyo Ardi Prabowo)

[kitagawa@is.t.kanazawa-u.ac.jp](mailto:kitagawa@is.t.kanazawa-u.ac.jp) (Akio Kitagawa)

\*Corresponding author

## INTRODUCTION

Hybrid electromagnetic solar energy harvesting (HES-ER) has become a promising solution to next-generation power of wireless communication, such as sensor nodes in wireless sensor networks and self-supporting Internet of Things (IoT) devices that recognize the latest research developments with energy harvesting techniques of radio frequency combining thin-film solar cells (Kim et al., 2019; Reynaud et al., 2017; Yuwono et al., 2015;). The HES-ER technique utilizes ambient and solar power to enable wireless devices to harvest solar and electromagnetic energy from RF signals (Pal et al., 2021). Ambient HES-ER is a green renewable energy solution that has attracted many researchers despite the great challenge of low incident power for the simultaneous and integrated design of HES-ER.

So, to increase the demanding requirements of the power ambient on the rectenna HES-ER system, research has been carried out for useful options regarding reliability and sustainability (Bahhar et al., 2020b; Wagih et al., 2021). The previous research has antennas with linear polarization, which are incapable of accommodating various polarizations caused by fading compared to CP antennas. Additionally, the antenna structure arrangement in the previous research did not mutually support the RF and solar energy harvesters, which are not situated in the same layer and have antenna impedance that needs to be matched (Mujahidin & Kitagawa, 2021a; Mujahidin & Kitagawa, 2021b).

This paper presents a hybrid electromagnetic solar energy harvesting design for ambient over a 2.3–2.4 GHz frequency band. It proposed a resonance structure-based matching stub. Circular polarization (CP) HES-ER strategically uses three layers of semiconductors to make up the antenna to achieve an axial ratio below 3 dB, a radiation pattern directional with many beams, and a relatively high gain (Hernowo et al., 2022; Hidayat et al., 2008). The integrated CP Antenna is exceptionally low-profile and compact, outperforming the existent HES-ER using a much more complex configuration. Furthermore, the applied array rectenna can be comfortably integrated into any embedded circuit board-based sensor device with mutually supporting performance layers in a single circuit board layer (Bahhar et al., 2020a; Bougas et al., 2021). More importantly, the simple design's overall circuit structure indicates that an antenna's impedance is tuned directly to serve a conjugate match with the impedance rectifier input in the expected working frequency under different input power and impedance matches between circuits (Mujahidin et al., 2020; Prasetya & Mujahidin, 2020).

## MATERIALS AND METHODS

### C-Slot CP Antenna HES-ER Sensor Circuit Design

The block diagram illustration of the C-Slot CP Antenna HES-ER Sensor Integrated Circuit

consists of a single circular antenna element with two output feeds connected linearly and directly to the sensor circuit and an energy harvester with an output impedance of 50 ohms (Figure 1). The configuration feed element uses a T-junction signal divider so that the CP antenna produced four outputs with the ability to harvest energy and produce phases with a 90-degree difference as a passive sensor element.

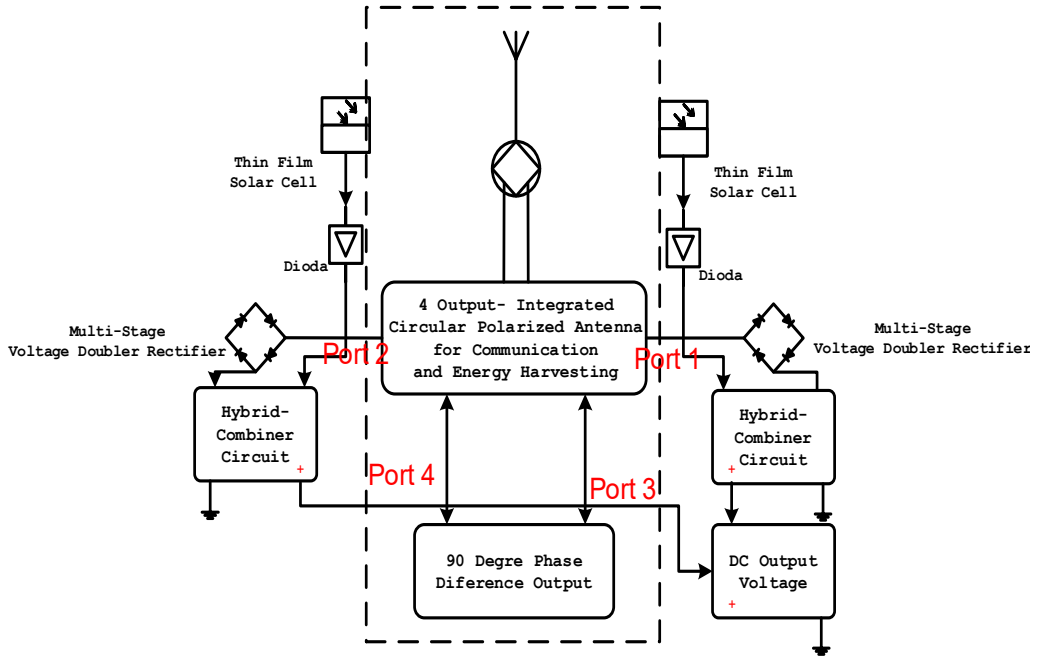


Figure 1. Block diagram of the circuit structure

The design of each component of the block considers the sustainability of the circuit with a model of one source of electromagnetic energy and two sources of solar energy. In the block diagram, the two solar sources take the position separately to show that the solar harvesting system still exists as a design with the antenna, but on the implementation of solar cells attached and integrated with the circuit C slot CP antenna (Bulu et al., 2006; Martinez et al., 2020). The connection between blocks can connect two models, the integrated circuit sensor and the SMA connector, on the energy harvesting system with a configured impedance matching.

### C-Slot CP Antenna

Design C Slot CP Antenna consists of two-line feeds that connect based on the optimization of the antenna with a circular patch to produce an AR of less than 3 dB to produce circular polarization. The circular patch configuration optimizes by shifting the position of the via as a feed connector around the disk side surface based on the propagation model calculations

on the antenna radiating element (Bai et al., 2020; Liu et al., 2018; Prasetya & Mujahidin, 2020). This optimization has the consequence of a continuous propagation change process on the disk surface so that symmetrically, the two probes can generate LHCP on the left and RHCP on the right. Add a C-slot antenna design to increase the sensitivity to circular polarization waves and optimize the antenna's working frequency. In our design, the receiving antenna's C slot and the asymmetric coupler circuits print on a single layer of partially grounded phenolic white paper substrate ( $\epsilon_r = 4.2$ ,  $\tan\delta = 0.0027$ ). The complete C-Slot CP Antenna-Integrated Asymmetric Coupler design is shown in Figure 2.

Optimizing the antenna's shape and ground dimensions in designing working frequency as antenna performance is a mathematical approach to shift the resonance frequency to patch and slot dimension changes. The mathematical approach of the C slot is one of the

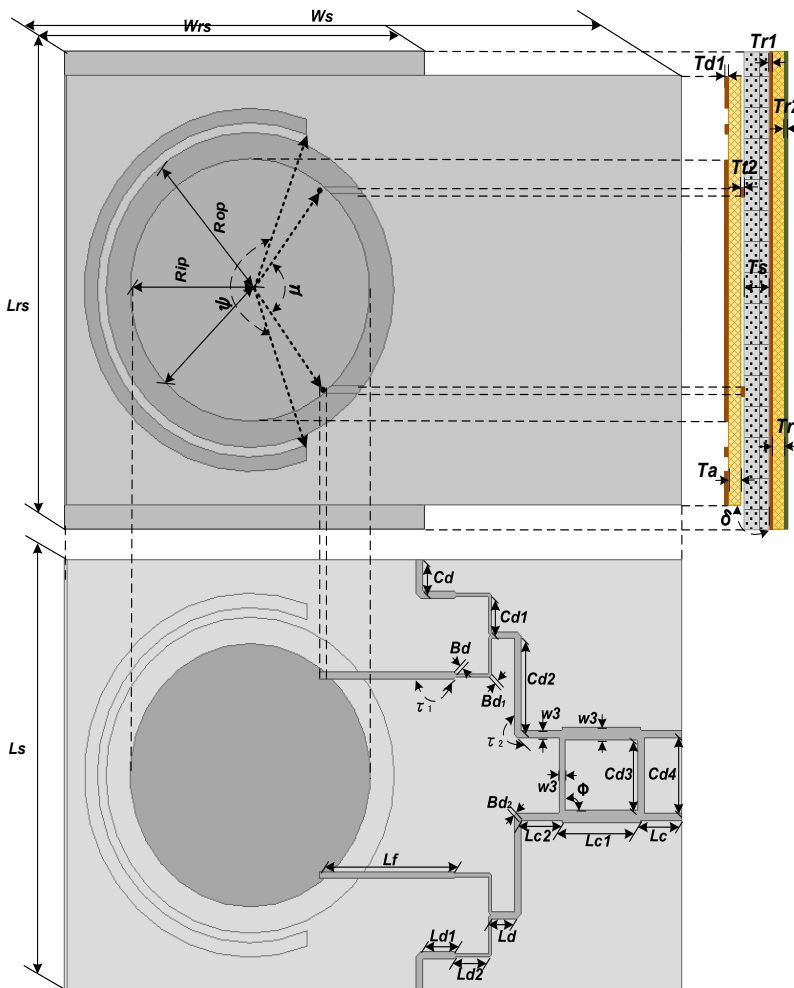


Figure 2. The structure design of C-slot CP antenna-integrated asymmetric coupler block diagram of the circuit structure

most crucial performance optimizations to improve accuracy and resonant frequency shift. The classification is based on the width of the slot dimensions and  $C_{St} = C_{so} - C_{si}$  to determine the distance between the inner and outer radius to the main patch with the slot position on the ground antenna. The slot dimension change accuracy is 0.0001 m with a tolerance value of 5%.

### Harvesting Circuit

The circuit harvesting configuration design optimizes by maximizing the available output power of the energy harvester by modeling the appropriate impedance at each transmission circuit. Therefore, the chosen design is a circuit voltage doubler proven effective in collecting RF and solar energy. So, as performance optimizes harvesters using a voltage multiplier, it is necessary to understand the stress multiplier process—the match of impedance between the harvester and the load. The harvesting part employing a stress multiplier applies the operation to the stress multiplier design with a freestanding inductive harvester based on the analysis design (Jones et al., 2018; Chen et al., 2022). It drives a monitoring sensor of wireless conditions using energy to extract from the magnetic field of ambient power frequency in an RF environment. The approximation of harvester calculation to the inductance  $L_{At}$  in step doubler with the resistance  $R_{At}$  in Figure 3 using the coil impedance. Analysis at the operating frequency  $F$ , where  $\omega = 2\pi f$  expresses the impedance in Figure 3.

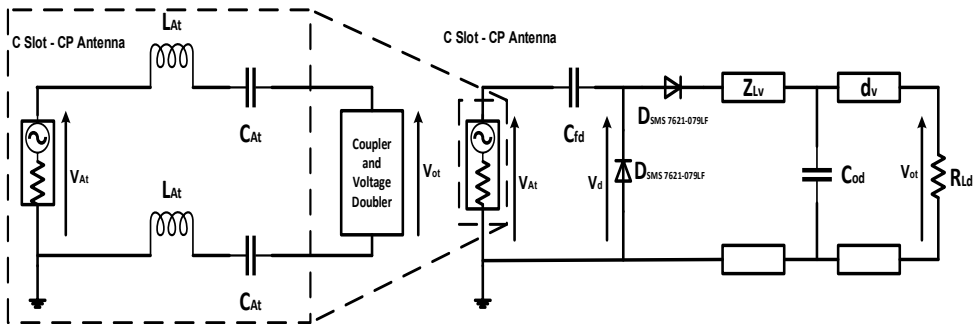


Figure 3. Harvester impedance of circuit configuration

This analysis applies to harvester designs using multipliers at the operating frequency in imaginary and real terms of components representing harvester impedance. An antenna is a source of AC voltage in ambient space, where at  $V_{At} = V_{in} \sin(\omega t - \theta)$ , in cycle with the impedance of coil impedance following Equation 1.

$$R_{At} + j\omega L_s \quad (1)$$

$V_{in}$  is the voltage of the open circuit that will turn up across the coil when positioned in the same magnetic domain; it is the frequency dominant in the magnetic domain through

which the antenna collects the energy and the phase shift between the harmonic base and the magnetic domain of the SMS 7750 Schottky diode. The series circuit with the antenna, Capacitor  $C_{At}$  has two roles: (1) it compensates for the self-inductance of the antenna, and (2) it is also in the multiplier circuit, which is the first capacitor. The  $C_{cp}$  is a connection of capacitor at the multiplier output to provide energy storage for the density of low magnetic periods flux while also serving as a capacitor of smoothing for the multiplier (Mitani et al., 2017; Mustafizur Rahman et al., 2020; Sonalitha et al., 2020).

The diode for the multiplier is the SMS 7750 Schottky diode, functioning as a low conduction loss. The harvester in Figure 4 provides power to the resistive load  $R_{Ld}$ , while the leak resistor  $R$  represents the leakage through  $D1, D2, C_{cp}$ , and parallel to  $R_{Ld}$ . It will also be the capacitance of the diode load, but this has an insignificant impact on the circuit's action as per the frequency specifications of the diodes, which is involved in most energy-harvesting multistage applications with the whole multistage circuit.

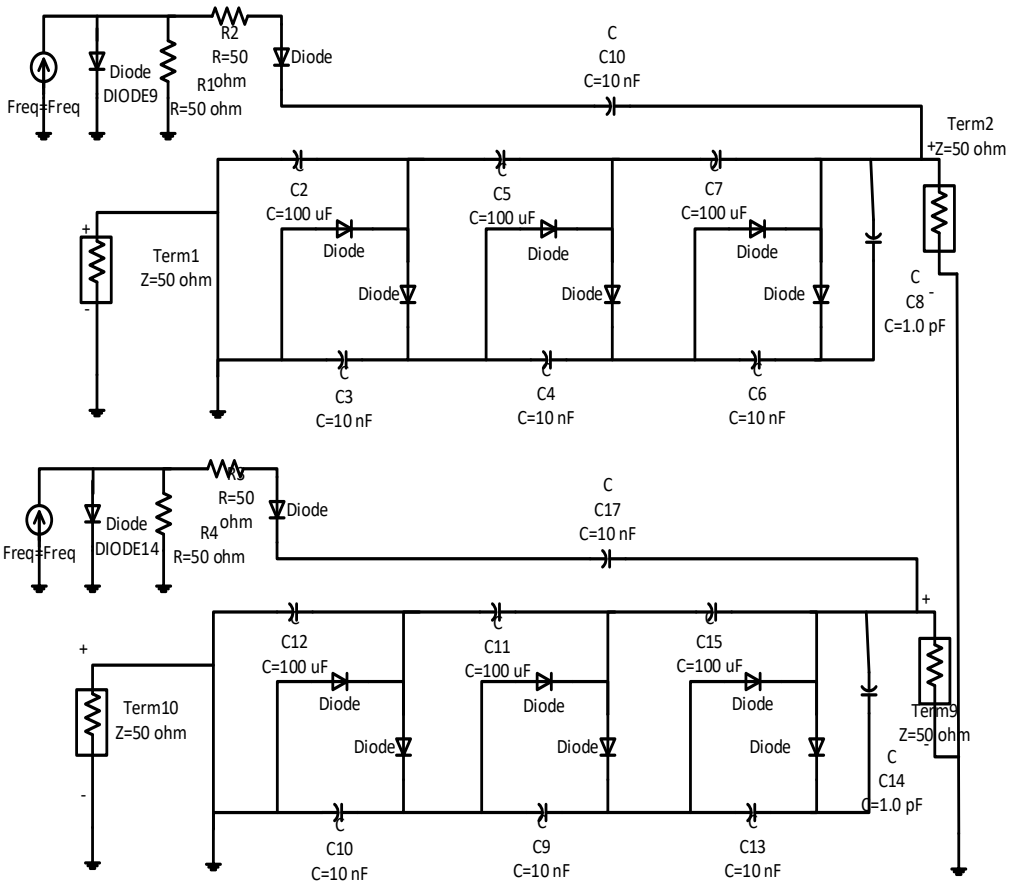


Figure 4. Harvesting multistage circuit configuration

The energy harvester in this work uses a 3-stage voltage doubler by accumulating in parallel with the coaxial connection with the solar cell integration (Figure 4). A single frequency dominates the design frequency in the circuit according to the antenna as a source with an AC harvesting source. Furthermore, in multistage operation, the AC surge harvester applied to a machine is dominated by a single band, although this band can often diverge with time. The output of the sine wave of the harvester goes to the voltage multiplier input. During the half-cycle negative, D1 establishes, so the voltage builds up on  $C_{At}$ .

During the half-cycle positive, the D2 charge transfers from  $C_{At}$  to  $C_{fd}$ . The circuit shows that both diodes cannot conduct simultaneously and will continue to increase to the next stage. The capacitor values are selected with values of  $100\mu\text{f}$  and  $10\text{pf}$ , so the charge time constant is much more extended than the input sine wave period (Bhattacharjee et al., 2018). Therefore, based on the analysis of the circuit construction method, determining the value of each component is based on the analysis in Figure 3, and then optimization is performed in the research to obtain the values of components that yield the highest power output (Mujahidin & Kitagawa, 2023).

To confirm the impedance output for the multiplier and the harvester, we analyze the circuit for an equilibrium state, where the power that will produce the harvester is equal to the power delivered to the RLd. With a magnetic flux density, the forward conduction loss in the SMS 7750 Schottky is a few W, in diversity to the loss between 10 W and a few mW. The diode conduction loss is therefore neglected in the analysis because it has a minimal value and is within the tolerance of the transmission voltage.

## RESULTS AND DISCUSSIONS

### C-Slot CP Antenna

A polarizing dual-feed C-Slot CP antenna with a configuration and a photo of the antenna fabrication is in Figure 5. The implementation of the optimized antenna configuration is in caption 1. The antenna size is  $37.8\text{ mm} \times 40.4\text{ mm} \times 1.6\text{ mm}$ . A feedline microstrip characteristic impedance of 50 excites the antenna. Four branches propagate RF-AC waves as sensors and harvest energy divided with the feedline. The four branches have the same width as the microstrip feedline with a T-junction configuration.

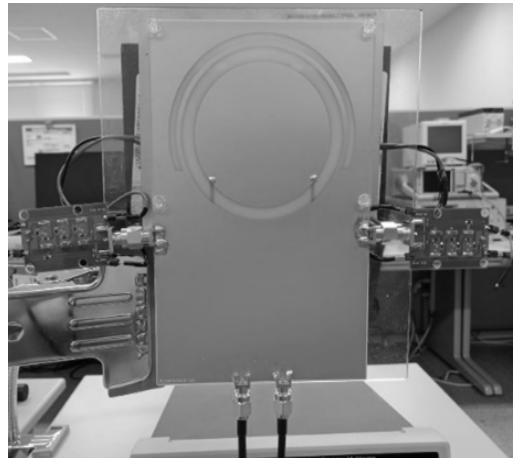


Figure 5. Fabrication of C-Slot CP antenna

The previous design report shows the impact of circular patch and C-slot parameters on characteristic impedance bandwidth. So, in this brevity, communication only discusses shorted vias and their effects on impedance matching and radiation characteristics. The antenna configuration was measured using Rhode and Schwarz ZVL Network Analyzer 9 KHz–13.6 GHz. The first is the characteristic impedance bandwidth of a dual-feed circular patch antenna and a C-slot with a via-hole connection in Figure 6. Bandwidth yields about 230 MHz (11%), about 2.4 GHz focus working frequency with a 2.35 GHz to 2.45 GHz frequency range.

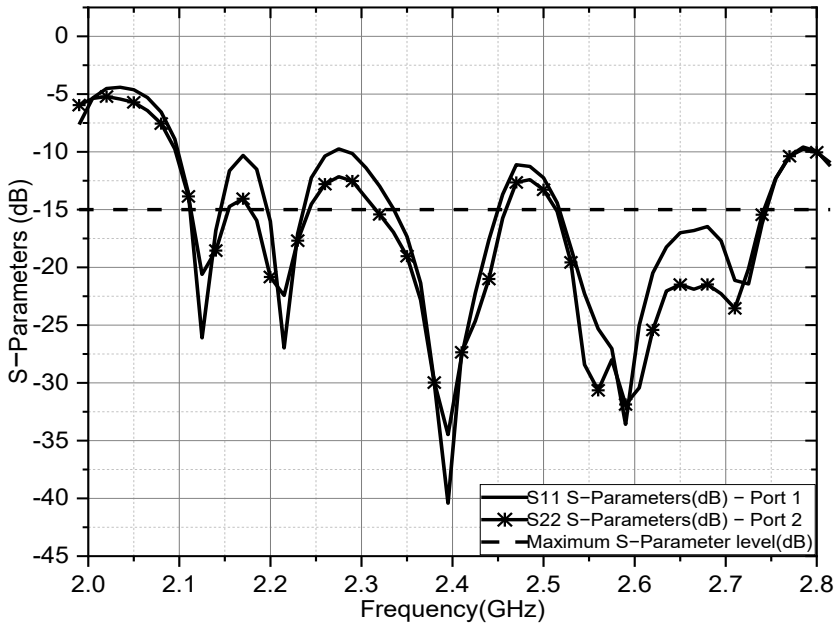


Figure 6. S parameter of C-slot CP antenna

The antenna element in the implementation has a symmetrical configuration to get a microstrip antenna with CP operation. Each fed and via hole position in this work is placed symmetrically to provide the wave propagation impulse needed to produce an axial ratio with a vertical and horizontal linear ratio below 3 dB. The proposed antenna's gain and axial ratio on antenna parameter results at the resonant frequency of 2.3–2.4 GHz in Figure 6. With an effective bandwidth of 24%, in Figure 7, the antenna exhibits complete coverage at the frequency range with  $AR < 3$  and a gain power level of 5.23 dB in the coverage field (Yuwono & Mujahidin, 2019; Zhang et al., 2022). The dual-feed configuration of a double C slot was developed to meet the requirements for impedance bandwidth, circular polarization features, 3 dB beamwidth with the dual feed technique, and antenna material with a low-cost profile.



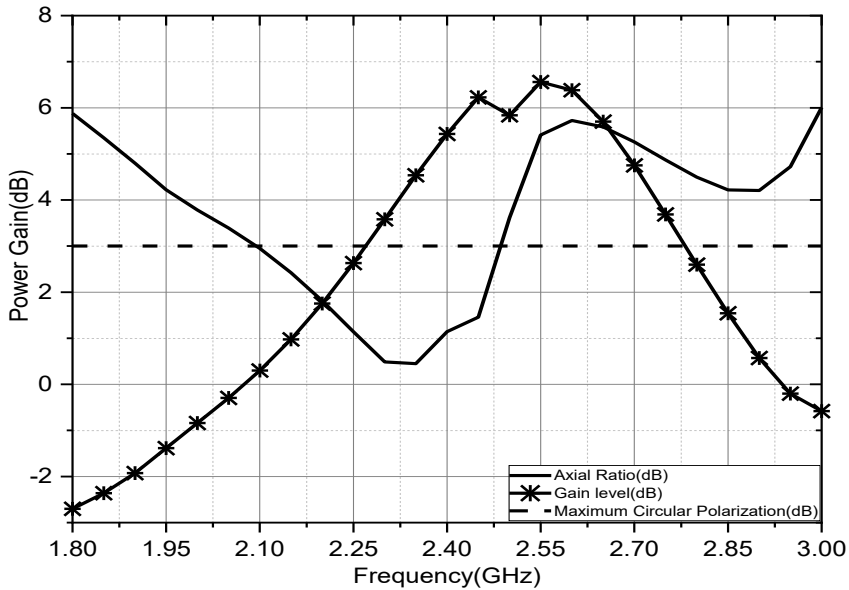


Figure 7. Gain level-axial Ratio of C-Slot CP antenna

### Stage Energy Harvester on Hybrid Electromagnetic Solar and Wireless Sensor

The test field produces periodic transmission of electromagnetic waves with different power levels with the same frequency, namely 2.4 GHz, so that the test configuration can represent the ambient propagation empirically with these variables. The spectrum levels are 9.57 dBm, 0.27 dBm, -8.4 dBm, -16.8 dBm, and -31.32 dBm. After setting up the spectrum level configuration, the thin-film solar cell test on the energy harvesting circuit needs to be measured as a simultaneous integration of two energy sources. Still, the solar cell test setup needs to be measured independently first to identify the process of generating solar energy on the circuit with a high level of illumination as the main variable to describe the ability of the voltage to stream in the circuit (O'Conchubhair et al., 2017; Yan et al., 2021). Figure 8 represents the light lumination value on thin-film solar cells' exposure to the output and electromagnetic integration.

Figure 8 shows a stable voltage increase with increasing luminance for solar energy generation. Then, it is essential to measure RF energy independently. RF energy radiates and transmits isotropically evenly in the area according to the test variable with maximum effectiveness of the propagation power level of 30 dBm in the test field. The energy harvesting circuit uses a configuration with a constant resistance value, so the main focus of testing is high power.

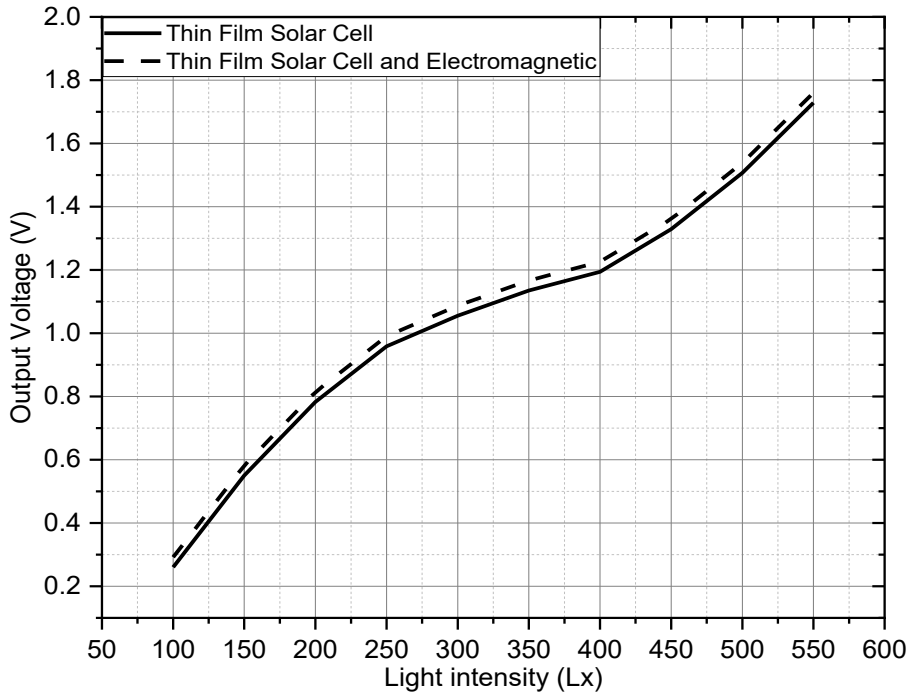


Figure 8. The light lumination value on thin-film solar cells' exposure to the output and electromagnetic integration.

## CONCLUSION

This study's compact C-slot CP antenna focuses on the structure and configuration of the new energy harvesting using hybrid electromagnetic solar in the wireless energy harvesting of ambient from low-power device sensors. The system configuration has a C-slot antenna with a circular patch dual-feed frequency band of 2.3–2.4 GHz. C-slot CP Antenna has a wideband circular polarized (CP) dual-feed adopted for axial ratio (AR) requirements, producing LHCP and RHCP and a 90-degree phase difference simultaneously during energy harvesting. The approximation function determines the variance of the output phase and magnitude of the feed configuration under the needed AR by examining the 50 Ohm feed configuration output characteristics for a dual feed CP antenna. The analysis shows that several branch channel couplers can individually attain an AR bandwidth of less than 3 dB, with a directional radiation pattern and a high gain value above 5 dBm, with an integrated reflector system optimization.

Furthermore, a high-frequency rectifier circuit embedded with a thin-film solar cell on the antenna then connects two rectifiers that divide the power T-junction to design an output voltage of high-efficiency DC. In the measurement and analysis of the configuration structure, the maximum voltage value is 1.76 V at the integrated source in the hybrid

solar electromagnetic harvesting configuration. With a compact energy harvesting and wireless sensor structure, to make a significant improvement to the wireless sensor system with a complete communication system-level analysis in an electromagnetic propagation environment using the multiple signal classification method of powered ambient RF energy, the independent sensor node demonstrates reliable operation in an indoor environment.

Therefore, it has significant implications for powering small electronics and wireless sensor applications independently of the IoT network or real-world telecommunications industry, so this prototype model is very efficient in energy harvesting using hybrid electromagnetic solar and wireless sensing processes. From this work, future research can be proposed in the form of increasing the power that can be produced by re-optimizing the voltage doubler circuit. In this research scheme, it is also necessary to carry out a more in-depth analysis regarding propagation analysis in communication networks apart from its function as energy harvesting.

## ACKNOWLEDGEMENTS

The authors acknowledge the financial, technical, and research support provided by the Graduate School of Natural Science and Technology, Kanazawa University, Japan and the Department of Telecommunication Engineering, Faculty of Electrical Engineering, Semarang State Polytechnic, Indonesia which made completing this work possible.

## REFERENCES

- Bahhar, C., Baccouche, C., & Sakli, H. (2020a). A novel 5G rectenna for IoT applications. In *2020 20th International Conference on Sciences and Techniques of Automatic Control and Computer Engineering (STA)* (pp. 287–290). IEEE. <https://doi.org/10.1109/STA50679.2020.9329349>
- Bahhar, C., Baccouche, C., & Sakli, H. (2020b). Optical RECTENNA for energy harvesting and RF transmission in connected vehicles. In *2020 17th International Multi-Conference on Systems, Signals and Devices (SSD)* (pp. 262–266). IEEE. <https://doi.org/10.1109/SSD49366.2020.9364243>
- Bai, B., Zhang, Z., Li, X., Sun, C., & Liu, Y. (2020). Integration of microstrip slot array antenna with dye-sensitized solar cells. *Sensors* 2020, 20(21), 6257. <https://doi.org/10.3390/S20216257>
- Bhattacharjee, A., Saha, S., Elangovan, D., & Arunkumar, G. (2018). Naturally clamped, isolated, high-gain DC–DC converter with voltage doubler for battery charging of EVs and PHEVs. In A. Garg, A. K. Bhoi, P. Sanjeevikumar & K. K. Kamani (Eds.) *Advances in Power Systems and Energy Management. Lecture Notes in Electrical Engineering* (pp. 439–450). Springer. [https://doi.org/10.1007/978-981-10-4394-9\\_44](https://doi.org/10.1007/978-981-10-4394-9_44)
- Bougas, I. D., Papadopoulou, M. S., Boursianis, A. D., Kokkinidis, K., & Goudos, S. K. (2021). State-of-the-Art Techniques in RF Energy Harvesting Circuits. *Telecom*, 2(4), 369–389. MDPI. <https://doi.org/10.3390/TELECOM2040022>
- Bulu, I., Caglayan, H., & Ozbay, E. (2006). Designing materials with desired electromagnetic properties. *Microwave and Optical Technology Letters*, 48(12), 2611–2615. <https://doi.org/10.1002/mop.21988>

- Chen, Q., Li, Z., Wang, W., Huang, Z., Liang, X., & Wu, X. (2022). A broadband dual-polarized solar cell phased array antenna. *IEEE Transactions on Antennas and Propagation*, *70*(1), 353–364. <https://doi.org/10.1109/TAP.2021.3098520>
- Hernowo, R., Suharjono, A., Supriyo, B., Mukhlisin, M., Hidayat, S. S., Wardihani, E. D., & K.K, S. B. (2022). Power consumption optimization for flood monitoring system using NB-IoT. In *2022 5th International Seminar on Research of Information Technology and Intelligent Systems (ISRITI)*, (pp. 58-63). IEEE. <https://doi.org/10.1109/ISRITI56927.2022.10052891>
- Hidayat, S. S., Kim, B. K., & Ohba, K. (2008). Learning affordance for semantic robots using ontology approach. In *2008 IEEE/RSJ International Conference on Intelligent Robots and Systems*, (pp. 2630–2636). IEEE. <https://doi.org/10.1109/IROS.2008.4651193>
- Jones, T. R., Grey, J. P., & Daneshmand, M. (2018). Solar panel integrated circular polarized aperture-coupled patch antenna for cubesat applications. *IEEE Antennas and Wireless Propagation Letters*, *17*(10), 1895–1899. <https://doi.org/10.1109/LAWP.2018.2869321>
- Kim, S., Tentzeris, M. M., & Georgiadis, A. (2019). Hybrid printed energy harvesting technology for self-sustainable autonomous sensor application. *Sensors*, *19*(3), 728. <https://doi.org/10.3390/s19030728>
- Liu, S., Hou, Y., Xie, W., Schlücker, S., Yan, F., & Lei, D. Y. (2018). Quantitative determination of contribution by enhanced local electric field, antenna-amplified light scattering, and surface energy transfer to the performance of plasmonic organic solar cells. *Small*, *14*(30), 1800870. <https://doi.org/10.1002/SMLL.201800870>
- Martinez, V. S., Jimenez, F. M., Baladron, I. P., Bautista, I. M., Ingelmo, J. V., Idoigabeitia, I. G., Besada, J. L., Iraguen, B. G., Gonzalez, J. M. F., & Mascarello, M. (2020). Steerable high-gain dual-reflector antenna at X-band for solar orbiter. *IEEE Transactions on Antennas and Propagation*, *68*(8), 5784–5795. <https://doi.org/10.1109/TAP.2020.2980333>
- Mitani, T., Kawashima, S., & Nishimura, T. (2017). Analysis of voltage doubler behavior of 2.45-GHz voltage doubler-type rectenna. *IEEE Transactions on Microwave Theory and Techniques*, *65*(4), 1051–1057. <https://doi.org/10.1109/TMTT.2017.2668413>
- Mujahidin, I., & Kitagawa, A. (2021a). CP antenna with  $2 \times 4$  hybrid coupler for wireless sensing and hybrid RF solar energy harvesting. *Sensors*, *21*(22), 7721. <https://doi.org/10.3390/S21227721>
- Mujahidin, I., & Kitagawa, A. (2021b). The novel CPW 2.4 GHz antenna with parallel hybrid electromagnetic solar for IoT energy harvesting and wireless sensors. *International Journal of Advanced Computer Science and Applications*, *12*(8), 393–400. <https://doi.org/10.14569/IJACSA.2021.0120845>
- Mujahidin, I., & Kitagawa, A. (2023). Ring slot CP antenna for the hybrid electromagnetic solar energy harvesting and IoT application. *TELKOMNIKA (Telecommunication Computing Electronics and Control)*, *21*(2), 290–301. <https://doi.org/10.12928/TELKOMNIKA.V21I2.24739>
- Mujahidin, I., Prasetya, D. A., Nachrowie, Sena, S. A., & Arinda, P. S. (2020). Performance tuning of spade card antenna using mean average loss of backpropagation neural network. *International Journal of Advanced Computer Science and Applications*, *11*(2), 639–642. <https://doi.org/10.14569/ijacsa.2020.0110280>

- Mustafizur Rahman, M., Krishno Sarkar, A., & Chandra Paul, L. (2020). A voltage dependent meander line dipole antenna with improve read range as a passive RFID tag. In H. S. Saini, R. K. Singh, M. Tariq Beg & J. S. Shambi (Eds.) *Innovations in Electronics and Communication Engineering. Lecture Notes in Networks and Systems* (Vol. 107, pp. 123–138). Springer. [https://doi.org/10.1007/978-981-15-3172-9\\_14](https://doi.org/10.1007/978-981-15-3172-9_14)
- O'Conchubhair, O., McEvoy, P., & Ammann, M. J. (2017). Dye-sensitized solar cell antenna. *IEEE Antennas and Wireless Propagation Letters*, *16*, 352–355. <https://doi.org/10.1109/LAWP.2016.2576687>
- Pal, P., Krishnamoorthy, P. A., Rukmani, D. K., Joseph Antony, S., Ocheme, S., Subramanian, U., Elavarasan, R. M., Das, N., & Hasanien, H. M. (2021). Optimal dispatch strategy of virtual power plant for day-ahead market framework. *Applied Sciences*, *11*(9), 3814. <https://doi.org/10.3390/APP11093814>
- Prasetya, D. A., & Mujahidin, I. (2020). 2.4 GHz double loop antenna with hybrid branch-line 90-degree coupler for widespread wireless sensor. In *10th Electrical Power, Electronics, Communications, Controls and Informatics Seminar* (pp. 298–302). IEEE. <https://doi.org/10.1109/EECCIS49483.2020.9263477>
- Reynaud, C., Duché, D., Palanchoke, U., Dang, F. X., Patrone, L., Le Rouzo, J., Gourgon, C., Charaï, A., Alfonso, C., Lebouin, C., Escoubas, L., & Simon, J. J. (2017). Harvesting light energy with optical rectennas. *Advanced Materials - TechConnect Briefs 2017*, *2*(2017), 45–48.
- Sonalitha, E., Zubair, A., Molyo, P. D., Asriningtias, S. R., Nurdewanto, B., Prambanan, B. R., & Mujahidin, I. (2020). Combined text mining: Fuzzy clustering for opinion mining on the traditional culture arts work. *International Journal of Advanced Computer Science and Applications*, *11*(8), 294–299. <https://doi.org/10.14569/IJACSA.2020.0110838>
- Wagih, M., Weddell, A. S., & Beeby, S. (2021). Powering e-textiles using a single thread radio frequency energy harvesting rectenna. *Proceedings*, *68*(1), 16. <https://doi.org/10.3390/PROCEEDINGS2021068016>
- Yan, N., Ji, C., Luo, Y., & Ma, K. (2021). A high gain solar cell aperture-coupled patch antenna based on substrate-integrated suspended line platform for 5G application. *Microwave and Optical Technology Letters*, *63*(11), 2876–2881. <https://doi.org/10.1002/MOP.33006>
- Yuwono, R., & Mujahidin, I. (2019). Rectifier using UWB microstrip antenna as electromagnetic energy harvester for GSM, CCTV and Wi-Fi transmitter. *Journal of Communications*, *14*(11), 1098–1103. <https://doi.org/10.12720/JCM.14.11.1098-1103>
- Yuwono, R., Mujahidin, I., Mustofa, A., & Aisah. (2015). Rectifier using UFO microstrip antenna as electromagnetic energy harvester. *Advanced Science Letters*, *21*(11), 3439–3443. <https://doi.org/10.1166/asl.2015.6574>
- Zhang, W., Liu, T., Yang, G., Jiang, C., Hu, Y., Zhu, X., Lan, T., & Zhao, Z. (2022). The application of beamforming technology in ionospheric oblique incidence sounding with Wuhan Multi-Channel Ionospheric Sounding System (WMISS). *IEEE Geoscience and Remote Sensing Letters*, *19*, 1–5. <https://doi.org/10.1109/LGRS.2021.3095910>